Chronic, wireless recordings of large-scale brain activity in freely moving rhesus monkeys

David A Schwarz[1,2], Mikhail A Lebedev[1,2], Timothy L Hanson[1,2], Dragan F Dimitrov[3], Gary Lehew[1,2], Jim Meloy[1,2], Sankaranarayani Rajangam[1,2], Vivek Subramanian[2,4], Peter J Ifft[2,4], Zheng Li[1,2], Arjun Ramakrishnan[1,2], Andrew Tate[1,2], Katie Z Zhuang[2,4] & Miguel A L Nicolelis[1,2,4–6]

Advances in techniques for recording large-scale brain activity contribute to both the elucidation of neurophysiological principles and the development of brain-machine interfaces (BMIs). Here we describe a neurophysiological paradigm for performing tethered and wireless large-scale recordings based on movable volumetric three-dimensional (3D) multielectrode implants. This approach allowed us to isolate up to 1,800 neurons (units) per animal and simultaneously record the extracellular activity of close to 500 cortical neurons, distributed across multiple cortical areas, in freely behaving rhesus monkeys. The method is expandable, in principle, to thousands of simultaneously recorded channels. It also allows increased recording longevity (5 consecutive years) and recording of a broad range of behaviors, such as social interactions, and BMI paradigms in freely moving primates. We propose that wireless large-scale recordings could have a profound impact on basic primate neurophysiology research while providing a framework for the development and testing of clinically relevant neuroprostheses.

Single-unit recordings from cortical neurons in awake, behaving monkeys were pioneered by Edward Evarts in the 1960s[1], paving the way for more than five decades of experimental studies focusing on the neurophysiology of the nonhuman primate's brain in action. Until the late 1990s, technological limitations allowed researchers to sample from just one neuron at a time or, in rare situations, from a few neurons simultaneously. The introduction of chronic multielectrode implants[1–4] and the development of computer technologies for online information processing and analysis allowed several advancements in the field of primate neurophysiology, such as recording simultaneously from many neurons for extended periods of time[5,6], extracting behavioral parameters from neural signals in real time[7], and using brain-derived signals to control external devices through BMIs[8,9]. Altogether, these developments transformed chronic brain implants into one of the most pervasive experimental approaches employed by systems neurophysiologists.

Because only tens of cortical neurons can be routinely sampled simultaneously in macaques (a miniscule fraction of the hundreds of millions of neurons that form the monkey cortex[10]), new neuronal recording methods are required to advance basic brain research, large-scale brain mapping and clinical translation of BMIs[11]. Furthermore, tethered recordings in experimental animals have limited the range of natural behaviors that can be studied, particularly in nonhuman primates. The transition to using a low-power, implantable, wireless interface is imperative for the success of experiments aimed at recording large-scale brain activity in behaving primates. In response to this need, several multichannel wireless recording systems have recently emerged[12–15]. However, to date, no system has been shown to be scalable in the number of recording channels.

Finally, considerable improvements in brain recording technology are needed before BMIs can become clinically relevant for helping severely disabled patients to regain mobility[11,16,17]. For example, our estimates indicate that a BMI aimed at restoring limb movements may require 5,000–10,000 neurons recorded simultaneously[18], whereas 100,000 neurons will be needed to drive a BMI in charge of producing full-body movements[17]. Here we introduce an integrated paradigm for chronic, multichannel, multisite, wireless large-scale recordings in freely roaming primates. We report the first volumetric recording probes with thousand-channel capacity, evidence of close to 5 years of continuous recordings, and the first scalable wireless recording interface validated in naturally behaving, unrestrained monkeys.

RESULTS

Chronic multichannel implants

Our results were obtained in eight adult rhesus monkeys (**Table 1**). Five monkeys received movable volumetric implants in multiple cortical areas of both cerebral hemispheres. Additionally, we present data from three rhesus monkeys (monkeys I, G and Cl) implanted with previous-generation microwire arrays composed of fixed (non-adjustable) microelectrodes. We also show the latest version of our movable volumetric implants, called recording cubes (**Fig. 1a**). We built each of these cubes by first creating an array of polyimide guiding tubes, spaced at 1 mm apart (4 × 10 or

[1]Department of Neurobiology, Duke University, Durham, North Carolina, USA. [2]Center for Neuroengineering, Duke University, Durham, North Carolina, USA. [3]Monterey Spine, Monterey, California, USA. [4]Department of Biomedical Engineering, Duke University, Durham, North Carolina, USA. [5]Department of Psychology and Neuroscience, Duke University, Durham, North Carolina, USA. [6]Edmond and Lily Safra International Institute of Neuroscience of Natal, Natal, Brazil. Correspondence should be addressed to M.A.L.N. (nicoleli@neuro.duke.edu).

RECEIVED 16 MAY 2013; ACCEPTED 12 MARCH 2014; PUBLISHED ONLINE 28 APRIL 2014; DOI:10.1038/NMETH.2936

Table 1 | Implant summary

Monkey	Channels implanted	Time with implant (months)	Max. units isolated	Units per microwire (global average)	Max. simultaneous channels (wired)	Max. simultaneous channels (wireless)	Refs.
O	1,792	13	1,874	0.522	512	N/A	This work
C	768	29	881	0.574	512	512	24
K	576	29	483	0.412	128	256	This work
M	384	54	490	0.640	384	128	22,23,36,37
N	384	54	357	0.465	384	N/A	22,23,36,37
I	160	20	224	0.698	128	N/A	38
Cl	160	12	77	0.240	128	N/A	20,29,39
G	128	7	114	0.448	128	N/A	20,29,39

10 × 10 arrangement). Each guiding tube accommodates bundles of 3–10 microwires of different length (**Fig. 1a**). Each bundle includes a single leading microelectrode with a conical tip; the remaining microwires have cut angle tips. We call these implants volumetric because they record from a volume of cortical (or subcortical) tissue (**Supplementary Fig. 1**). The microelectrodes are made of stainless steel microwires, 30–50 µm in diameter, with polyimide insulation that leaves the tip exposed. The guiding tubes are fixed in a 3D-printed plastic case, which also holds miniature screws for positioning the microelectrodes. The resulting recording cubes are light and compact: a fully assembled unit weighs 11.6 g and has a surface area per channel of ~0.22 mm^2. A total of 4–8 recording cubes can be implanted per monkey (**Supplementary Fig. 2**).

During an implantation surgery, the guiding tube array is fixed in light contact with the cortical surface, without penetrating the brain. Several days later, the microwire bundles are advanced into the cortical tissue by rotating a set of microscrews. Depending on the design, each microscrew turn advances microelectrodes housed in one (**Supplementary Fig. 3**) or several guiding tubes (**Fig. 1a**). In our previous work with fixed arrays, the microelectrodes were inserted in the cortex during surgery, and although these implants were less durable than our moveable arrays, histology performed on animals with these arrays showed little damage to cortical layers[6] (**Supplementary Fig. 4**). Using movable arrays, we have learned that penetration with subsets of microelectrodes reduces dimpling of cortical surface and copes with the 'bed of nails effect', which often hinders simultaneous penetration by many microelectrodes in traditional arrays and silicon probes. In our implantation approach, each microelectrode bundle is lowered gradually over the course of several days. This allows microelectrodes to be positioned more slowly and also much more deeply into the cortical tissue (i.e., layer VI).

Additionally, because our chronic cortical recordings have lasted for close to 5 years in our monkeys (see below), it is likely that our implantation paradigm also maintains healthier cortical tissue.

After the recording cubes are fixed in place with dental cement, a custom-designed 3D-printed headcap is added to the implant to provide protective housing for the microelectrodes and electronics (**Fig. 1c**,**d**). The headcap is fitted in a modular manner. First, a conical base module is fixed on the top of the skull, which protects the implants and their connectors. Depending on the application, several additional modules can be attached to this base to accommodate electronics. For example, a wireless-compatible module houses radio transceivers and their power source (**Fig. 1d**). Omnetics 36-pin connectors are employed to connect both external cables and the wireless headstages. For all monkeys except monkey O, the connectors were fixed with dental cement in between the cubes (**Fig. 1b**). For monkey O, implanted with 1,792 microwires, a special module organized all connectors (**Fig. 1c**).

Multichannel recordings

Monkeys M and N were the first animals to be implanted with four recording cubes containing 96 microwires each (totaling 384 microwires per monkey). The cubes were placed bilaterally in the primary motor (M1) and primary somatosensory (S1) cortices, (**Supplementary Fig. 2**). Then, using a more compact revision, we implanted six cubes bilaterally in the arm and leg representation areas of monkey K's M1 and S1, totaling 576 channels.

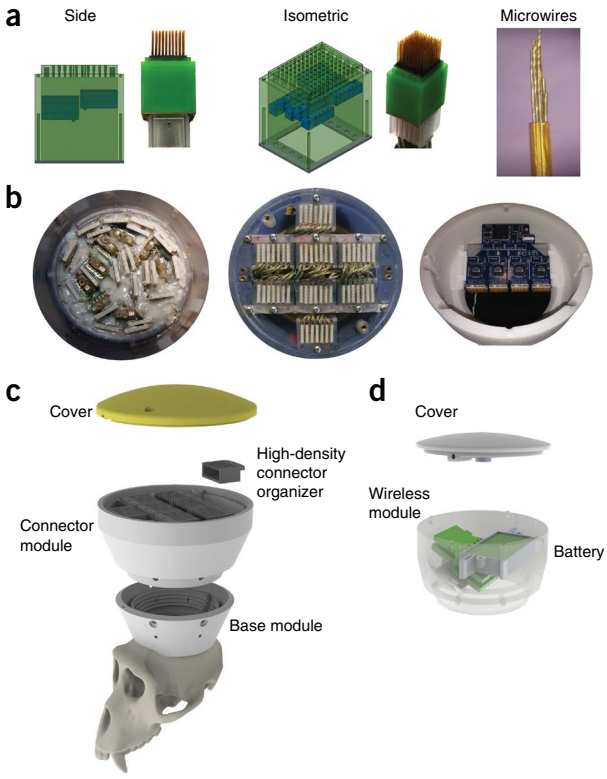

Figure 1 | Recording cubes and primate headcap. (**a**) Schematics and photographs of actual microwire cubes, showing the wire density and adjustment mechanisms. The third generation is a 10 × 10 array that is fitted with bundled microwires. (**b**) Photographs of final arrangements of connectors, showing the top of the headcap of a monkey implanted with second-generation cubes (left) and a similar view of the large-scale brain array module on a monkey implanted with third-generation cubes (center). Right, wireless module mounted on the headcap. (**c**) Layered schematic showing the modular headcap assembly, with the large-scale brain array connector organizer as the active module. (**d**) Schematic showing the modular headcap wireless assembly. Both headcaps are 3D printed.

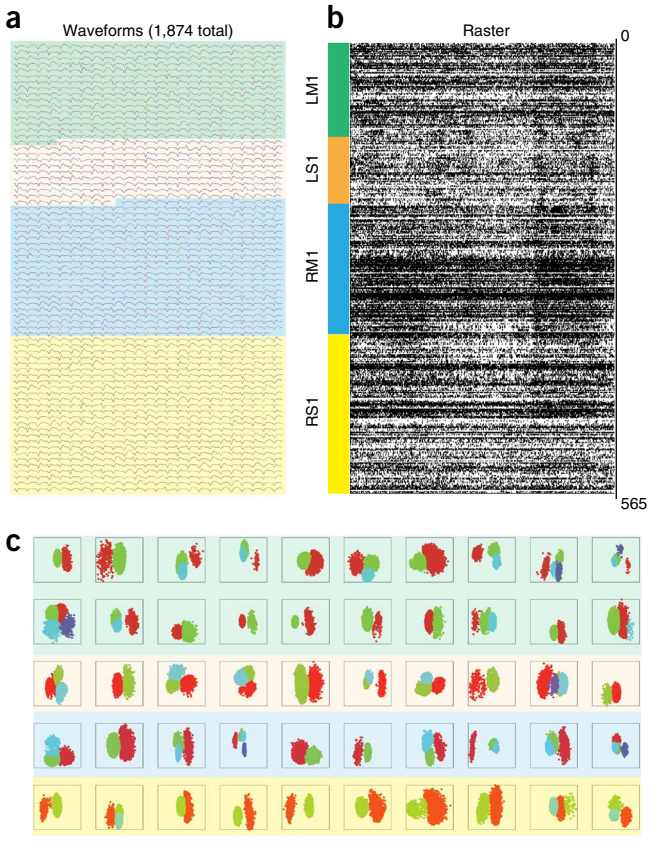

Figure 2 | Large-scale activity recordings. (**a**) Representative mean waveforms for 1,874 neurons over a center-out task. Coloring indicates the array of origin: green, left-hemisphere primary motor cortex M1 (LM1); orange, left-hemisphere primary somatosensory cortex S1 (LS1); blue, right-hemisphere M1 (RM1); yellow, right-hemisphere S1 (RS1). (**b**) Population raster plot depicting a 1-s window of neuronal spiking activity for a single recording session (565 neurons). The vertical color key identifies the recorded areas. A 128-channel Plexon system was used for each recorded area. (**c**) Unit isolation clustering using the first two principal components of a subset (50) of channels from monkey O. Each color in the plots represents labeling of individual unit principal-component analysis clusters. Colored shading indicates the array of origin as in **a**.

Monkey C was implanted with eight of these recording cubes, bilaterally in the supplementary motor area (SMA), M1, posterior parietal cortex (PPC), dorsal premotor cortex (PMd) and S1, totaling 768 channels (**Supplementary Fig. 5**). The latest revision allowed us to implant four 448-channel cubes, containing a total of 1,792 microelectrodes, in four cortical areas (448 microwires in each area, S1 and M1 in both hemispheres) of monkey O. One month after the original implantation surgery, extracellular neuronal recordings were obtained from these implants through four 128-channel recording systems (Plexon) (**Fig. 2a**,**b**), for a total of 512 channels recorded simultaneously. A total of 1,874 single cortical units were isolated in monkey O at the end of four consecutive daily recording sessions (each day recording 512 channels). 968 units were recorded in M1 (left hemisphere, 403; right hemisphere, 565), and 906 units were recorded in S1 (left hemisphere, 254; right hemisphere, 652) (**Fig. 2b**,**c**).

Long-term recordings

The longevity of our implants was assured through sterile surgery performed by an experienced neurosurgeon, regular (1-mm) spacing between implanted guiding cannulas, and slow insertion of microelectrodes into the brain. In this sample, monkeys I, Cl and G had older-generation fixed arrays, whereas monkeys M, N, C, K and O had the movable recording cubes. Altogether, this approach has yielded high-quality neuronal recordings from eight rhesus monkeys. To our knowledge, our recordings[6,17–24] supersede the longevity reported with silicon probes[25] or any other method thus far. This finding is further illustrated by a 4-year (2009–2013) sample of neuronal waveform traces, obtained from monkeys M and N (**Fig. 3**). At the time of writing, the recording duration in these animals has reached close to 5 years. Additionally, we have been recording from monkeys K and C (both females) for over 29 months. Monkey O (female), implanted with the most advanced arrays, has been recorded from for 13 months. We recorded from monkeys I, Cl and G for 20, 12 and 7 months, respectively. Generally, the average yield (**Fig. 3** and **Table 1**) for stable implants remained around 0.5–1.0 units (over time) per microwire, a value that agrees with our previous results obtained

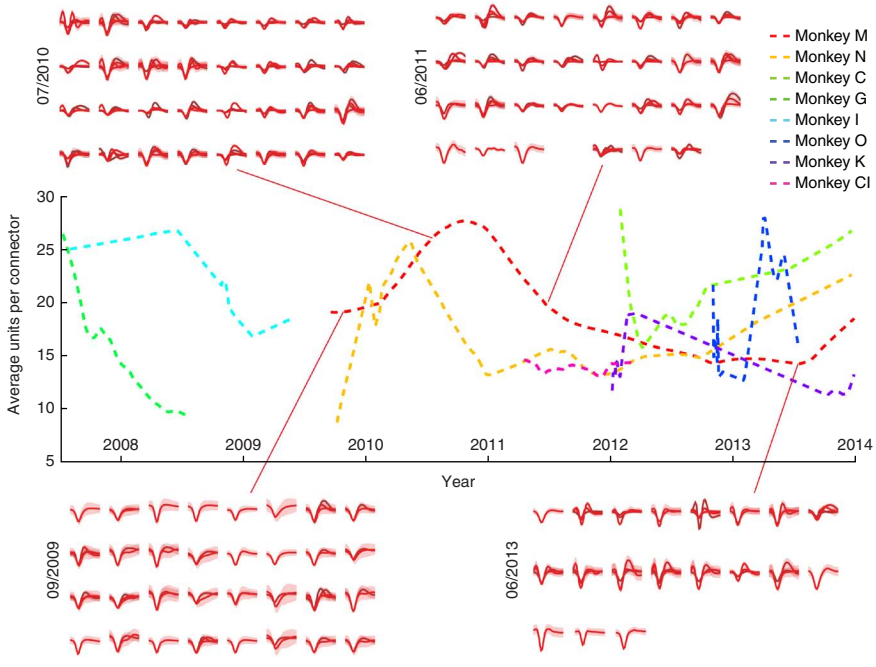

Figure 3 | Recording longevity. Neuronal recording yield over time measured by quantifying the average number of single units recorded per connector (32 channels). All the data from the five monkeys used in these experiments, and from three other monkeys (G, I and Cl), were used. Four-year sample waveforms, identified by date, from monkey M's left-hemisphere M1 connector, surround the figure. Lines represent mean sample waveforms, and shaded areas correspond to the waveform's s.d. These are taken from a single session on the corresponding date.

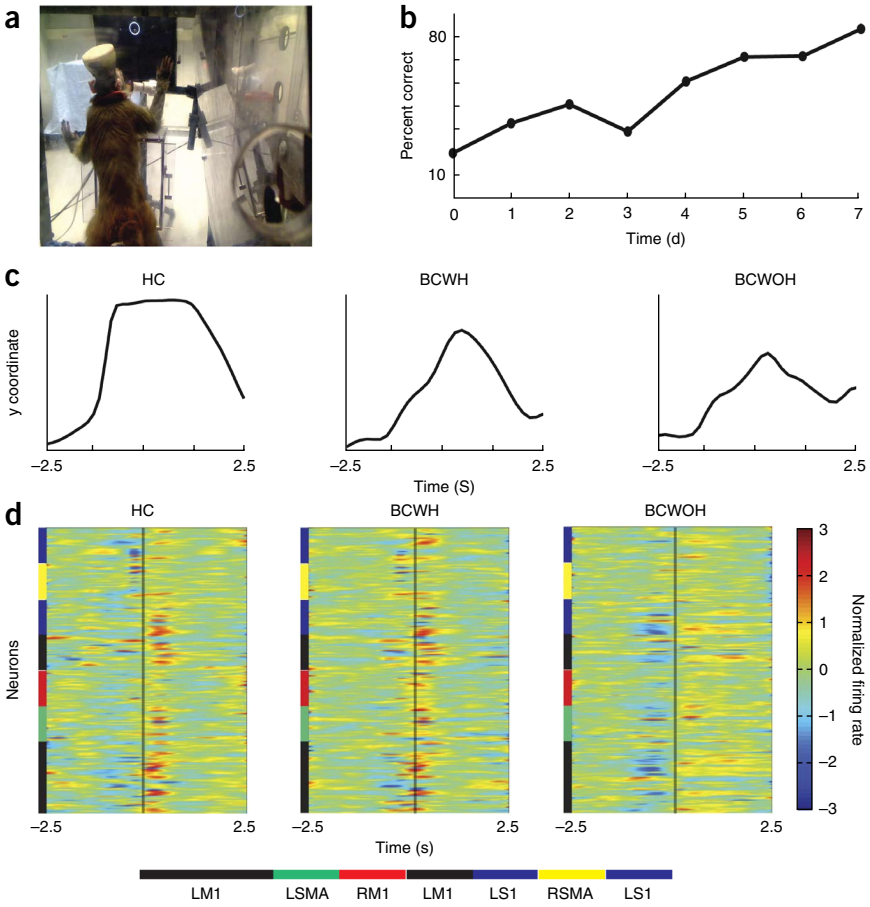

Figure 4 | Wireless brain-machine interface (monkey C data). (**a**) Monkey with wireless system performing a task using pure brain control (**Supplementary Video 1**). (**b**) Performance metric increase in a single week of training for a single monkey. (**c**) Example average traces for the *y* coordinate of the cursor for trials with a target at 0° (north) of orientation, showing average constant movements despite variable postures during task interaction, as well as time to target. Peaks indicate reached target. (**d**) Peri-event time histograms centered on target onset for 212 units, grouped at each column with cursor control paradigms of basic hand control (HC) with joystick, brain control with joystick (BCWH) and sole brain control (BCWOH). The color key shows unit groupings per area. Each unit was normalized per condition using the *z*-score method. RSMA, right-hemisphere supplementary motor area.

using adaptations of this methodology in rodents[4] and human patients[26,27].

Large-scale data processing

Processing large-scale data sets is a computationally demanding task. To handle real-time operations, we had to develop routines to process continuous streams of neural data and behavioral parameters. We also had to find a way to scale the number of neural channels. We solved the first issue by developing a real-time BMI suite (**Supplementary Table 1**)—a software package written in C++ for the Windows platform—that implemented all basic components needed to process large-scale activity and route it to control external devices (**Supplementary Fig. 6**). For the second issue of input scaling, we developed approaches for both tethered and wireless recordings. In our tethered recordings, which sample the full waveform of all channels, we developed networked spike acquisition software, which aggregated spikes acquired from multiple computers. In our wireless recordings, the system was designed to obtain waveform samples solely at the start of the session, when spike sorting parameters were generated. This enabled considerable scaling owing to the low bandwidth used.

Wireless recording system

Our wireless recording system was designed to match typical BMI needs (**Supplementary Table 2**). This system consists of four components: digitizing headstages, a wireless transceiver, a wireless-to-wired bridge and client software (**Supplementary Figs. 7–9**). Four such headstages are attached to a transceiver module for a total of 128 channels per transceiver unit (31.25 kHz sampling per channel, 1.3 kHz sampling of spike time onset). Multiple 128-channel modules can be stacked together to scale up the final system. Our system's novel feature, bidirectional communication, enables spike sorting to be performed on the transceiver itself, thereby saving both power and wireless bandwidth. This is accomplished through key elements of the transceiver: the radio and the digital signal processor (DSP). The DSP performs signal conditioning, spike sorting and radio control to match the radio bandwidth with the 48-Mbps aggregate rate of data acquisition. Each transceiver is powered by a 3.7-V, 2,000–mA h lithium-ion cell and consumes approximately 2 mW per channel, or ~264 mW per 128-channel unit, allowing continuous operation for over 30 h. The wireless-to-wired bridge takes incoming radio packets and bridges them with an Ethernet interface. Overall, this signal chain is optimized in both temporal and power domains, allowing for the increased number of channels. Additionally, because of the low bandwidth requirements, each transceiver uses a small slice of the industrial, scientific and medical (ISM) radio band. This allows substantial scaling on the number of recording channels. We benchmarked our wireless system performance using four transmitters, or 512 channels simultaneously, by measuring packet-bit drop errors (PER/BER) versus transmission range. Overall, the system performed within its optimal range (3 m) with all four modules (**Supplementary Fig. 10a**). We then used this 512-channel system to record brain activity while monkey C reached for grapes. Out of the 512 wirelessly recorded channels, we isolated a total of 494 units (103 M1 units, 102 S1 units, 98 SMA units and 191 PPC units). Cortical units exhibited typical firing-rate modulations as the animals produced arm-reaching movements (**Supplementary Fig. 10b**). For other experimental validation, we used two transceivers per monkey (i.e., 256 channels).

Wireless brain-machine interface

The real-time operation of our wireless system in a typical BMI setup was tested in monkey M (128 channels in one group of

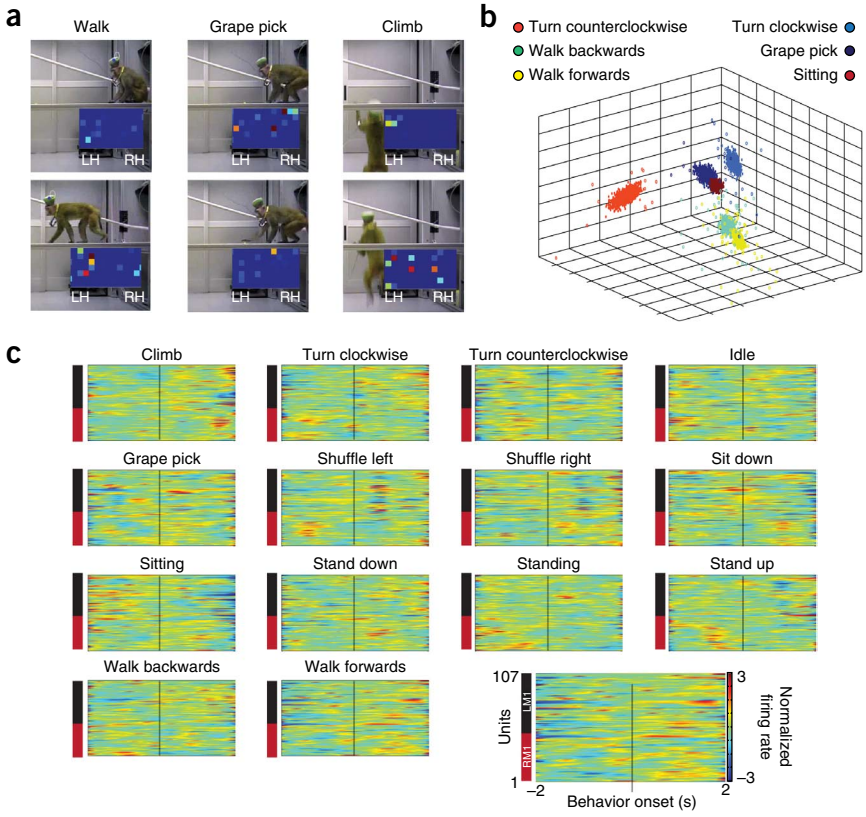

Figure 5 | Recordings of freely behaving monkeys. (**a**) Screenshots from videos used for coding of behaviors. Two frames each for three sample behaviors are shown. See **Supplementary Video 3**. (**b**) First three principal components of neural activity for six different behaviors in monkey K. Principal-component analysis data were used for support vector machine classification (see **Supplementary Table 3**). (**c**) Peri-event time histograms for behaviors from monkey K, calculated from 107 M1 neurons and centered around behavior onset. The spectrogram legend is on the bottom right. Each unit was normalized for the entire session (all behaviors shown) using the *z*-score method.

experiments, and 256 in the other), monkey C (256 and then 512 channels) and monkey K (256 channels). These monkeys performed several BMI and behavioral tasks without any restraint. While inside a large Plexiglas enclosure (**Fig. 4a**), monkeys C and M learned to use their brain activity to move a computer cursor to execute a classical center-out task (Online Methods). Initially monkey C used a joystick to perform the task manually (the HC, or 'hand control', condition). Monkey C was then required to perform through a BMI, with a Wiener filter used as the decoder[28]. During the 'brain control with hand' condition (BCWH), the joystick was still accessible to the monkey, although it was disconnected from the cursor control. During 'brain control without hand' (BCWOH), we removed the joystick from the setup, forcing the monkey to perform the task using its cortical activity alone (**Supplementary Video 1**). A total of 212 cortical units recorded from M1 (84 and 26 units in the left and right hemispheres, respectively), SMA (27 and 24 units) and left hemisphere S1 (51 units) were used. Performance improved (reaching >80% correct trials) within 7 d (**Fig. 4b**). Population peri-event time histograms (PETHs) for all recorded neurons, centered on target onset, show neuronal adaptation to each task component (**Fig. 4**). Cortical ensembles exhibited similar patterns of modulation in BCWH and HC, periods during which the animal moved the joystick. Different neuronal modulation patterns were observed in BCWOH, likely owing to decreased body movements. In particular, many units were prominently inhibited before target onset. Additionally, excitatory neuronal modulations occurred during reaching for all modes of operation but had lower amplitude and longer duration during BCWOH. We then replicated this task using a powered wheelchair as an end effector (**Supplementary Video 2**).

To address the relevance of the number of recording channels for BMI decoding, we conducted an offline analysis known as neuron-dropping curves[7] by randomly removing units from the training set of the decoder (unscented Kalman filter[29]). The performance of the decoder was measured as the correlation coefficient (*r*) between decoded and measured variable. We show neuron-dropping curves for two monkeys (O and C) performing the center-out task and for two monkeys (M and N) performing a bipedal locomotion task on a treadmill (**Supplementary Fig. 11**). For all tasks and monkeys, model performance increased linearly as a function of the logarithm of the total number of neurons[18].

Wireless recordings in freely moving monkeys

We also explored the capacity of our wireless system to record from freely moving monkeys in an exploratory foraging task. Monkeys K and C were allowed to freely move about an experimental room (**Supplementary Video 3**) while picking grapes from locations on the room floor and on suspended planks. Recordings included a total of 247 units from monkey C (193 in M1; 64 in S1) and 156 units from monkey K (107 in M1; 49 in S1). Our wireless system recorded reliably inside the 3-m range of the recording equipment (**Fig. 5a** and **Supplementary Video 2**). Population PETHs aligned on the onset of different behaviors showed distinct neuronal modulation patterns (**Fig. 5c**). We then used several clustering methods (*k*-means, expectation maximization and support vector machines (SVMs; linear kernel and radial basis function)) to discretely classify several observed behaviors. All four clustering methods employed yielded good performance (**Supplementary Table 3**) in correctly identifying six selected behaviors (**Fig. 5b**) on the basis of the combined electrical activity of cortical ensembles.

We did further experimental validation with monkey K while it performed an unrestrained locomotor task. The monkey walked both bipedally and quadrupedally on a treadmill while we wirelessly recorded from 176 units in M1 (left hemisphere, 94; right hemisphere, 82). Population PETH analysis of left M1 neurons during the swing phase of the right ankle revealed an inversion of firing patterns in a subpopulation of these cells (**Supplementary Fig. 12**).

Next-generation implants

Continuous improvement of our arrays is necessary to further explore the relevance of large-scale recordings in BMIs and neurophysiology. We have introduced a manufacturing modification (**Supplementary Fig. 13a**,**b**) that allows us to increase the number of microelectrodes per individual cannula in our recording cubes to up to 30 microwires and a new cap that accommodates close to 10,000 microwires (**Supplementary Fig. 13c**,**d**).

DISCUSSION

To meet future experimental demands, chronic multielectrode implants should fulfill the following requirements: (i) produce minimal damage to neural tissue, (ii) maximize the number of simultaneously recorded neurons, (iii) sample from multiple brain areas, and (iv) maintain good recording quality for several years. Over the last two decades, our laboratory has progressively improved the performance of multichannel recording systems, moving toward these goals through a series of technological developments and experimental tests in rodents, primates and humans (via intraoperative recordings)[26,30,31]. Here we described a paradigm that allows wireless large-scale brain recordings to be carried out in freely roaming primates.

The first step of this paradigm involved the introduction of volumetric recording probes, which can be used to sample from hundreds to thousands of neurons, distributed across multiple cortical areas per monkey. Using this integrated methodology, we increased the number of cortical units recorded simultaneously per monkey in a single recording session (~500 units)[24], the total number of units isolated from a single animal (~2,000 units) and the longevity of chronic recordings (close to 5 years). To our knowledge, none of these milestones has been reached by another integrated system for chronic recordings in behaving monkeys. For comparison, the Utah silicon probe, commonly used for BMI studies and other neurophysiological experiments in primates, provides fewer recording channels (~100), penetrates only the superficial cortical layers, does not allow adjustment of the microelectrode's position after the implantation surgery, and cannot yield long-term cortical recordings beyond a few months[25,32].

The large increase in the number of neurons recorded has not compromised the stability and reliability of our implants. Although we have not performed histology for the most recent implants, we have previously shown that implanted microwires produce minimal tissue damage[33]. This is further demonstrated by the fact that high-quality neuronal data could be recorded from two monkeys for nearly 5 years and in another two monkeys for nearly 3 years. Although neuronal yield decreases between the first and third after the surgery, we showed that recordings stabilize at an average of 0.5–1.0 units per channel for many months or even years in most monkeys. A similar yield has been observed over the past 20 years in our laboratory in the recordings from rodents[4], owl monkeys[7] and human subjects[26,27].

Moreover, the performance of BMI decoders increases linearly with the logarithm of the cortical neuronal sample recorded simultaneously[18]. Therefore, increasing the number and long-term stability of multielectrode recordings is imperative for the development of clinically relevant neuroprostheses driven by BMIs. Indeed, we have recently employed the technology described here to implement the first bimanual BMI, which used approximately 500 units to control a pair of virtual arm actuators[24]. We envision that by doubling or tripling the sample of neurons recorded simultaneously, even richer BMI applications, such as a robotic exoskeleton aimed at restoring full-body mobility, may become viable.

Previously, our group[14] and other laboratories[12,13,15] have described multichannel wireless recording technologies. Although most of these systems improved the design, size, energy efficiency and depth of implants of the components (**Supplementary Table 4**), our current approach introduces several notable innovations. The key innovation is its ability to maintain bidirectional wireless communication, an essential property missing in the literature. Bidirectional wireless communication is a crucial component for scaling up the number of channels recorded simultaneously, as it allows spike sorting to be performed on the implant and, therefore, reduces the amount of information transferred wirelessly. Using this approach, we recorded up to 512 channels of neuronal data in the present study. Overall, considering only the ISM band, we estimate that in the future, up to 20 128-channel transceivers could be used, each occupying 2-MHz increments, for a total of 2,560 recording channels. Because two neurons could be isolated per channel, this technology could yield up to 5,120 neurons recorded simultaneously in a single monkey. However, a few bottlenecks, including size and power consumption, must be addressed before this benchmark can be reached.

Additionally, removing the need for hardware tethering is extremely advantageous for primate experiments, particularly when there is growing evidence that the context in which animals perform a given task dramatically influences the physiological properties of neural circuits[28]. For example, studies focused on how cortical circuits underlie natural behaviors such as tool utilization, social primate interactions and complex movements[34,35] are likely to benefit from our new recording paradigm.

Use of a novel wireless large-scale recording approach as described here may prove ideal for studies of large-scale brain activity under a variety of normal and pathological conditions, and it may serve as both the neurophysiological and technological backbone for the development of future generations of BMIs and clinical neuroprostheses.

METHODS

Methods and any associated references are available in the online version of the paper.

Note: Any Supplementary Information and Source Data files are available in the online version of the paper.

ACKNOWLEDGMENTS

Awards from the US National Institute of Mental Health (NIMH) DP1MH099903 and the US National Institute of Neurological Disorders and Stroke (NINDS) R01NS073952 to M.A.L.N. supported this research. We thank L. Oliveira and T. Phillips for their gracious support during all implantation surgeries and experimental logics. Additionally, many thanks go to S. Halkiotis for her continued help in the manuscript revision and submission process. We also thank T. Vinholo for performing the extensive histology that is shown in this work and H. Powell for analyzing video data from the free roaming experiment.

AUTHOR CONTRIBUTIONS

D.A.S., M.A.L. and M.A.L.N. designed experiments and wrote the paper. D.A.S., V.S., M.A.L. and M.A.L.N. analyzed data. D.A.S., M.A.L., S.R., A.R., P.J.I., A.T., T.L.H. and K.Z.Z. performed the experiments. D.A.S., J.M. and G.L. designed and constructed animal headcaps and manufactured wireless units. G.L. designed and constructed the microwire recording cubes. D.A.S. and T.L.H. wrote the wireless software. T.L.H. designed and constructed the wireless system. T.L.H. and Z.L.

wrote the BMI software and contributed analysis code. D.F.D. designed and performed the surgical procedures.

COMPETING FINANCIAL INTERESTS

The authors declare no competing financial interests.

1. Evarts, E.V. Pyramidal tract activity associated with a conditioned hand movement in the monkey. *J. Neurophysiol.* **29**, 1011–1027 (1966).
2. Nicolelis, M.A.L., Lin, R.C.S., Woodward, D.J. & Chapin, J.K. Induction of immediate spatiotemporal changes in thalamic networks by peripheral block of ascending cutaneous information. *Nature* **361**, 533–536 (1993).
3. Supèr, H. & Roelfsema, P.R. Chronic multiunit recordings in behaving animals: advantages and limitations. *Prog. Brain Res.* **147**, 263–282 (2005).
4. Nicolelis, M.A.L., Ghazanfar, A.A., Faggin, B.M., Votaw, S. & Oliveira, L.M.O. Reconstructing the engram: simultaneous, multisite, many single neuron recordings. *Neuron* **18**, 529–537 (1997).
5. Nicolelis, M.A.L. Actions from thoughts. *Nature* **409**, 403–407 (2001).
6. Nicolelis, M.A.L. *et al.* Chronic, multisite, multielectrode recordings in macaque monkeys. *Proc. Natl. Acad. Sci. USA* **100**, 11041–11046 (2003).
7. Wessberg, J. *et al.* Real-time prediction of hand trajectory by ensembles of cortical neurons in primates. *Nature* **408**, 361–365 (2000).
8. Chapin, J.K., Moxon, K.A., Markowitz, R.S. & Nicolelis, M.A.L. Real-time control of a robot arm using simultaneously recorded neurons in the motor cortex. *Nat. Neurosci.* **2**, 664–670 (1999).
9. Nicolelis, M.A.L. & Lebedev, M.A. Principles of neural ensemble physiology underlying the operation of brain-machine interfaces. *Nat. Rev. Neurosci.* **10**, 530–540 (2009).
10. Azevedo, F.A.C. *et al.* Equal numbers of neuronal and nonneuronal cells make the human brain an isometrically scaled-up primate brain. *J. Comp. Neurol.* **513**, 532–541 (2009).
11. Marblestone, A.H. *et al.* Physical principles for scalable neural recording. *Front. Comput. Neurosci.* **7**, 137 (2013).
12. Chestek, C.A. *et al.* HermesC: low-power wireless neural recording system for freely moving primates. *IEEE Trans. Neural Syst. Rehabil. Eng.* **17**, 330–338 (2009).
13. Bonfanti, A. *et al.* A multi-channel low-power system-on-chip for single-unit recording and narrowband wireless transmission of neural signal. *Conf. Proc. IEEE Eng. Med. Biol. Soc.* **2010**, 1555–1560 (2010).
14. Rizk, M. *et al.* A fully implantable 96-channe 96-channel neural data acquisition system. *J. Neural Eng.* **6**, 026002 (2009).
15. Borton, D.A., Yin, M., Aceros, J. & Nurmikko, A. An implantable wireless neural interface for recording cortical circuit dynamics in moving primates. *J. Neural Eng.* **10**, 026010 (2013).
16. Lebedev, M.A. & Nicolelis, M.A.L. Brain-machine interfaces: past, present and future. *Trends Neurosci.* **29**, 536–546 (2006).
17. Lebedev, M.A. *et al.* Future developments in brain-machine interface research. *Clinics (Sao Paulo)* **66** (suppl. 1), 25–32 (2011).
18. Lebedev, M.A. & Nicolelis, M.A.L. Toward a whole-body neuroprosthetic. *Prog. Brain Res.* **194**, 47–60 (2011).
19. Lebedev, M.A. *et al.* Cortical ensemble adaptation to represent velocity of an artificial actuator controlled by a brain-machine interface. *J. Neurosci.* **25**, 4681–4693 (2005).
20. Lebedev, M.A., O'Doherty, J.E. & Nicolelis, M.A.L. Decoding of temporal intervals from cortical ensemble activity. *J. Neurophysiol.* **99**, 166–186 (2008).
21. Zacksenhouse, M. & Nemets, S. in *Methods for Neural Ensemble Recordings* 2nd edn. (ed. Nicolelis, M.A.L.) Ch. 4 (CRC Press, 2008).
22. O'Doherty, J.E. *et al.* Active tactile exploration enabled by a brain-machine-brain interface. *Nature* **479**, 228–231 (2011).
23. Shokur, S. *et al.* Expanding the primate body schema in sensorimotor cortex by virtual touches of an avatar. *Proc. Natl. Acad. Sci. USA* **110**, 15121–15126 (2013).
24. Ifft, P.J., Shokur, S., Li, Z., Lebedev, M.A. & Nicolelis, M.A.L. A brain-machine interface enables bimanual arm movements in monkeys. *Sci. Transl. Med.* **5**, 210ra154 (2013).
25. Lu, C.W., Patil, P.G. & Chestek, C.A. Current challenges to the clinical translation of brain machine interface technology. *Int. Rev. Neurobiol.* **107**, 137–160 (2012).
26. Patil, P.G., Carmena, J.M., Nicolelis, M.A.L. & Turner, D.A. Ensemble recordings of human subcortical neurons as a source of motor control signals for a brain-machine interface. *Neurosurgery* **55**, 27–35, discussion 35–38 (2004).
27. Hanson, T.L., Fuller, A.M., Lebedev, M.A., Turner, D.A. & Nicolelis, M.A.L. Subcortical neuronal ensembles: an analysis of motor task association, tremor, oscillations, and synchrony in human patients. *J. Neurosci.* **32**, 8620–8632 (2012).
28. Carmena, J.M. *et al.* Learning to control a brain-machine interface for reaching and grasping by primates. *PLoS Biol.* **1**, E42 (2003).
29. Li, Z. *et al.* Unscented Kalman filter for brain-machine interfaces. *PLoS ONE* **4**, e6243 (2009).
30. Nicolelis, M.A.L. Brain-machine interfaces to restore motor function and probe neural circuits. *Nat. Rev. Neurosci.* **4**, 417–422 (2003).
31. Nicolelis, M.A.L., Lehew, G.C. & Krupa, D.J. Miniaturized high-density multichannel electrode array for long-term neuronal recordings. US patent 6,993,392 (2006).
32. Maynard, E.M., Nordhausen, C.T. & Normann, R.A. The Utah Intracortical Electrode Array: a recording structure for potential brain-computer interfaces. *Electroencephalogr. Clin. Neurophysiol.* **102**, 228–239 (1997).
33. Freire, M.A.M. *et al.* Comprehensive analysis of tissue preservation and recording quality from chronic multielectrode implants. *PLoS ONE* **6**, e27554 (2011).
34. Ochsner, K.N. & Lieberman, M.D. The emergence of social cognitive neuroscience. *Am. Psychol.* **56**, 717–734 (2001).
35. Mattout, J. Brain-computer interfaces: a neuroscience paradigm of social interaction? A matter of perspective. *Front. Hum. Neurosci.* **6**, 114 (2012).
36. O'Doherty, J.E., Lebedev, M.A., Li, Z. & Nicolelis, M.A.L. Virtual active touch using randomly patterned intracortical microstimulation. *IEEE Trans. Neural Syst. Rehabil. Eng.* **20**, 85–93 (2012).
37. Ifft, P.J., Lebedev, M.A. & Nicolelis, M.A.L. Cortical correlates of Fitts' law. *Front. Integr. Neurosci.* **5**, 85 (2011).
38. Fitzsimmons, N.A., Lebedev, M.A., Peikon, I.D. & Nicolelis, M.A.L. Extracting kinematic parameters for monkey bipedal walking from cortical neuronal ensemble activity. *Front. Integr. Neurosci.* **3**, 1–19 (2009).
39. O'Doherty, J.E., Lebedev, M.A., Hanson, T.L., Fitzsimmons, N.A. & Nicolelis, M.A.L. A brain-machine interface instructed by direct intracortical microstimulation. *Front. Integr. Neurosci.* **3**, 20 (2009).

ONLINE METHODS

Animals. All animal procedures were performed in accordance with the US National Research Council's Guide for the Care and Use of Laboratory Animals and were approved by the Duke University Institutional Animal Care and Use Committee. Five adult rhesus macaque monkeys (*Macaca mulatta*; one male, four females) participated in the set of experiments (monkeys M, N, C, K and O). Additionally, data from three monkeys (Cl, G and I; two males, one female) were used in the longevity analyses. Histology data from one additional monkey (T, one female) were used in this report.

Surgery. Adult rhesus macaques were initially anesthetized with ketamine and then intubated in the trachea. They were then placed in a stereotaxic apparatus and ventilated. General anesthesia was maintained with isoflurane throughout the surgery. A series of craniotomies were performed over the stereotaxically determined locations of cortical areas of interest. The dura mater was removed, and sulci landmarks were inspected to confirm the location of cortical areas. Microwire cubes were brought in light contact with the pia mater and fixed to the bone with bone cement. Titanium screws were inserted in the skull to anchor the cement. Gelfoam coated in saline was inserted into the pia to sustain the surrounding tissue. After all recording cubes were implanted, a protective headcap was affixed to the screws and cemented to the skull. The cap encased the cubes and their connectors and provided housing for wireless components. The dura, dense connective tissue and, later, skull tissue grow back to capture and seal each of the microelectrode array/bundle penetration point. We have observed such tissue restoration in all implanted monkeys examined post-mortem. Because of these processes, the risk of infection growth around the microelectrode implants decreases substantially over the first few weeks after the implantation surgery.

Implantation. Once the animals recovered from the surgery (usually 1 week post operation), we began the insertion of the microelectrodes. The potential for infection is vastly reduced during the first post-surgery week by using antibiotic gel to cover the entire implant. Following the surgery and array implantation, microwire bundles were inserted slowly into the brain. Each microelectrode bundle was moved gradually over the course of several days. This was achieved by turning microscrews in the array assembly, which lowered subsets of microwires independently. Each quarter turn of the microscrew lowers the bundle by 53 μm. As expected, microelectrodes did evoke a tissue reaction over the first few weeks after implantation. This tissue reaction, which included a local immunological response, was contained and did not lead to any significant tissue damage outside the microelectrode penetration rack.

Implants. Because the cortices of rhesus monkeys are convoluted, the implants were developed to be suited for both relatively shallow penetrations in cortical gyri and deeper penetrations in the sulci. As such, our recording cubes contain guiding tubes loaded separately for gyri and for sulci. For gyral penetrations, guiding tubes are fitted with 2–5 microelectrodes staggered at 0.3–0.5 mm. For sulcal penetrations, 5–10 microelectrodes are staggered at 0.5–1.0 mm. Using this approach, the density of microelectrodes within a cortical volume can be adjusted, depending on the depth of the targeted cortical area. Monkeys M and N were implanted with four 96-microwire recording cubes constructed of stainless steel 304 (30–50 μm in diameter). Each hemisphere received two cubes: one in the upper-limb representation area and one in the lower-limb representation area of sensorimotor cortex. Monkeys C and K were implanted with 128-microwire cubes (stainless steel 304, 30–50 μm in diameter). Monkey K received two cubes in M1 and one array in S1 for each hemisphere. Monkey C received two cubes in M1, one in S1 and another in SMA. Monkey O was implanted with four 448-channel cubes (stainless steel 304, 30–50 μm in diameter), one in M1 and one in S1 for each hemisphere. Data from three previous monkeys (monkeys I, Cl and G) were used for longevity analysis. Monkeys I, Cl and G were implanted with 96-microwire arrays. Histology data from one additional monkey (T) was used in this report. Monkey T was implanted with three 32-microwire (stainless steel 304, 50 μm in diameter) fixed arrays.

Neuronal isolation. After electrode insertion, we examined each microwire for units and made adjustments to the cortical depth of the wire on the basis of these results. After microwire positioning, we performed spike sorting for use in our experiments, monitoring the units on an almost daily basis (**Supplementary Videos 4** and **5**). Units were sorted using standard template-matching paradigms[40] available in our Plexon and wireless recording systems, which are standard and well used across the literature[16]. To assess whether recorded units were single or multiple, we estimated refractory period using interspike intervals. Units that exhibited refractory periods greater than 1.6 ms (ref. 9) were considered single units. Population plots included data from both single units and multiunits, so recorded units in these plots will be referred to simply as 'neural units' or 'units'.

Histology. Histology for microelectrode tracts was performed in one animal (monkey T). The animal was deeply anesthetized with pentobarbital and transcardially perfused with 4% paraformaldehyde. Sections of representative areas of interest of the brain were selected, prepared and stained with cresyl violet (Nissl method) in order to identify electrode track locations. Slices were prepared using a HMH 505 E cryostat (Microm) with 50-μm thickness.

BMI suite. Our BMI suite is written in C++ and DirectX 9.0. It uses Lua bindings for configuration and scripting, and it interfaces directly with Plexon using the C++ Plexon API. The BMI suite also interfaces with our custom-designed wireless system using a remote procedural call (RPC) service written in the wireless client that transmits the firing rate of all neurons at every request (the BMI RPC calls at 100 Hz). Interfacing with other data streams is usually achieved through a UDP socket or, less often, a simple serial interface. Other signal input sources may be added in the future, using all existing algorithmic methods, without significant modification of the existing infrastructure because of the modularity of the design. Decoding algorithms operate using a common interface with the BMI software suite, allowing new routines to be implemented in a modular way. Algorithmic outputs can be combined flexibly at the user's behest using the software's GUI and then passed to the experiment manager module. The experiment subroutine implements the behavioral task and handles stimuli, feedback and experimental procedure logic. The experiment manager

doi:10.1038/nmeth.2936

module uses a standardized interface, which allows different experiments to be switched in and out without affecting the rest of the software suite. Finally, experimental data are recorded through a unified threaded logging system, which automatically records all pertinent experimental variables.

Wireless transceiver. An Analog Devices Blackfin BF532 DSP performs signal conditioning, sorting and radio control on the transceiver and is written in assembly language. The Blackfin processor uses sum absolute accumulate (SAA) instructions, typically used in MPEG video compression, in order to implement L1 norm template sorting. The analog-to-digital converters (ADCs) output four samples every microsecond, and processing each proceeds in lockstep. First they are dithered to 14 bits via a low-pass prefilter, high passed at 250 Hz via an integrator, and then gained further from 0–128 (7.8 fixed point) with a 1-bit stochastic automatic gain control (AGC) block. This is followed by a 1-bit-normalized least mean squares (LMS) adaptive noise cancellation wherein the last 14 circular-buffered sampled channels are used to linearly predict the present channel. Then this prediction is subtracted, and the error is saturated to 1 bit (plus sign) and used to update the weights. Only one weight is updated at a time, but as noise is largely uncorrelated with this rate (2.232 kHz), it does not affect the rejection ratio of >40 dB. Noise-canceled samples are fed to eight poles of host-configurable IIR biquads, implemented as Direct Form-I with coefficient prescaling to prevent fixed-point saturation. The biquads are implemented with ping-pong register buffering and share taps between subsequent stages for maximum efficiency. Importantly, these biquads can be configured as oscillators, which has proved useful when debugging radio function.

On each headstage, a 32-channel amplifying and multiplexing chip (Intan RHA2132) feeds a 12-bit ADC (ADCS7476; 31.25 kHz sampling on each channel). Digital signals are isolated from the analog inputs with LDO regulators.

The Blackfin processor has a special SAA instruction that is intended to speed MPEG video compression by measuring the block difference between frames; here we use it to rapidly implement L1 norm template-based sorting. As the SAA instruction operates on a four-sample 32-bit word, samples from each of the four headstages are shortened to 8 bits and merged into one word and placed into a circular buffer; the sum of absolute differences of 16-sample stretches of waveform are then computed and compared to a threshold. If they are below the threshold, a spike is marked as detected via a sticky bit in a radio FIFO. Two such templates are implemented per channel (templates A and B) for a total of 256 templates per unit. Note that there is no other threshold operation; template matching for both units per channel is computed for every incoming sample.

Wireless transmission uses a Nordic Semiconductor radio (nRF24L01+; 2.4GHz; 2 Mbps unidirectional bandwidth; 1.333 Mbps with overhead and direction switching). Signal conditioning occurs in synchrony to radio control, as there are no threads on the system; radio control state is implicitly encoded in the program counter. Radio data are sent as cyclic redundancy check (CRC)-protected 32-byte packets at a rate of 5,208.3 packets/s; the radio control code fills these packets with six samples from each of four continuously transmitted channels, plus 8 bytes of template match. This equates to all 256 bits of template match being transmitted at 1.3 kHz. However, this packet leaves no space for synchronization or acknowledgment communication. Accordingly, given that L1 template matching is unable to accurately detect two simultaneous action potentials (templates A and B), we drop a few of these unlikely events via a lookup table compression, freeing up one extra bit per byte in the template-match fields. Four such bits are used to synchronize the transceiver and bridge, as every 16 outgoing packets the transceiver transitions to receive a command packet. The other 4 bits are used as an echo field to verify command-packet reception. This radio protocol, including state transitions, utilizes 99.6% of available bandwidth with the Nordic radio chip. The whole transceiver software, which is written in assembly, fully processes a sample in less than 80 instructions and consumes only 12.6 kB of L1 cache.

Wireless bridge. Rather than using polarized antennas, the bridge uses three identical Nordic radios with orthogonally arranged antennas; radio packets are accepted from any source provided they match the CRC. Successful reception of a data packet transitions the receiving radio to transmit mode and begins bidirectional communication. There are four pairs of addresses and data, which allow all elements of the signal conditioning path to be varied on the transceiver, for example, to set template, vary bandpass filter, disable AGC or set which channels are being continuously transmitted. The bridge also features a full protocol stack, including IP, ICMP, DHCP, TCP, HTTP and SLP, the last of which allows software discovery of bridges. Finally, the bridge features audio output, transceiver programming circuitry, and a power-over-Ethernet (PoE) module, so it can be remotely powered, for example, within an animal room.

Wireless client. The sorting client is written in C/C++ using the GTK2 GUI toolkit with OpenGL and HLSL for graphics, presently on Debian GNU/Linux. The software allows further GUI control of all elements of the signal-conditioning path, as outlined above. The client software allows for direct visualization of waveforms from four selected channels and all spike channels, while enabling spike sorting, data collection, signal chaining, and interfacing with multiple bridges and transceivers. For spike sorting, two units can be sorted per channel, for a maximum of 256 units per transceiver. Unit isolation and sorting is performed with an algorithm based on principal component analysis (PCA): the user specifies a threshold to obtain waveform snippets, which are then represented by the first two principal components on a 2D plane. The user then marks the clusters of dots that represent neuronal waveforms in the PCA space. This software will be available upon request, and will be available in the near future as open source (as well as the wireless hardware) under GPL v3.

Unrestrained center-out task. The task requires placing a computer cursor in the middle of the screen and, upon the appearance of a target, placing the cursor over the target for a juice reward. Each trial commenced with a circular target appearing in the center of the screen. The monkeys held the cursor within this target for a delay randomly drawn from a uniform distribution (from 500 to 2,000 ms). After this delay, the central target disappeared and a circular target appeared on the screen at a distance of 7 cm from the center, in one of eight directions. The spacing between the objects was 0.1 cm. Before this task was run inside the Plexiglas enclosure,

animals were trained while seated in a primate chair. The enclosure was large enough (1 m × 1 m × 1 m) to allow the monkeys freedom of movement. The monkeys were free to perform the task at any time and accommodated to the enclosure quickly. In only 3 d, they started performing the manual task. Monkeys' behavior was captured throughout each session by a video camera. For the long-term tasks, data collection was done by running an Ethernet PoE cable from a laboratory computer to the home cage and replacing the wireless system's batteries every 24 h.

Locomotion task. Three monkeys were involved in locomotion studies (M, N and K). They were trained to walk bipedally on a custom-modified treadmill. A standard neck restraint was suspended from a linear actuator, which allowed bipedal support to be adjusted gradually while the monkey achieved bipedal posture and weight bearing. A juicer was placed in front of the macaque and could be raised or lowered depending on the macaque's height and the locomotor task (bipedal or quadrupedal walking). A video monitor mounted in front of the monkey displayed visual feedback for tasks, training and enrichment. Only monkey K used wireless recordings and walked quadrupedally. Monkey M and N walked only bipedally and were recorded with our Plexon system, and their results were used in the dropping-curve analysis.

Powered wheelchair. A conventional motorized wheeled chair was modified for computer-controlled movements. The human chair was dismounted, and the wheeled base was interfaced with a Robotics motor controller (RoboteQ Model VDC2450) based on a dual-channel microprocessor. Computer control was established using a 900-MHz serial pipe (APC, Wireless RS232) to transmit serial commands from the computer to the controller at a rate of 9,600 baud.

Wheelchair task. Using the protocol for the center-out task, we applied data from the cursor in both BCWH and BCWOH paradigms as input into a differential-drive control law that was used to drive the wheelchair through the room (3 m × 3 m × 4 m). An additional cursor was shown on the screen, which represented the wheelchair following the monkey's cursor position. To provide this additional feedback, the wheelchair's coordinates were video tracked and transformed onto the screen. Additional rewards were administered when the wheelchair cursor hit the target. The algorithm of wheelchair control set the linear and angular velocities of the wheelchair as functions of the monkey cursor position, and programmable boundaries kept the wheelchair from striking the walls by setting linear velocity to 0 when outside the boundary of the working area. A sample video of the task is shown in **Supplementary Video 2**.

Free roaming experiments. Monkey K was videotaped, and 256 cortical units were simultaneously recorded in this animal while it roamed freely in a room (3 m × 3 m × 4 m). Offline, the monkey's motions were hand labeled into 15 categories of behavior. Neuronal data were aligned with video recording; neurons that did not fire over 500 times in 1 h were eliminated (leaving 107 neurons), and PETH analysis was performed with 2-s windows and 100-ms bins. Population PETH data were calculated and analyzed as spectrograms. For discrete predictions, six behaviors were selected on the basis of their saliency and ease of identification, as well as the amount of data available to them (>30 events per behavior).

Kinematics tracking. An in-house–developed tracking system was used to track the three-dimensional position of the ankle, knee, hip, wrist, shoulder and head of monkeys, as well as the surface of the limbs. Both limbs were tracked using two units of this system.

Decoding algorithms. Historically, BMI research has used Weiner filters for online predictions of movement. Recently in our laboratory, we developed a more advanced algorithm for predicting limb movements, called the unscented Kalman filter[29]. This algorithm was used for the extraction of lower-limb kinematic parameters from cortical activity, as well as cursor parameters from joystick tasks. The Weiner filter was also applied when indicated. For discrete classification, we used Matlab implementations of EM, SVM and *k* means.

Analysis. All data analyses were performed on Matlab. No investigator blinding, nor animal randomization, was performed. PETHs were calculated taking a 1-s time window centered on target onset in the joystick tasks, or swing onset for the left leg in the locomotor tasks, and averaging binned firing rates over all trials for each neuron. Neuron activity was normalized per neuron, per condition. Analysis of recordings over months and years of experimentation was performed by script, reading all experimental files and counting average number of units recorded per 32-channel array. For behavioral clustering, we used implementations of PCA, EM, SVM and *k* means available in the Matlab statistical toolbox. Analysis of neuron scaling performance was done by using all neurons, then randomly removing subsets and then cross-validating the process over several iterations.

40. Lewicki, M.S. A review of methods for spike sorting: the detection and classification of neural action potentials. *Network* **9**, R53–R78 (1998).

doi:10.1038/nmeth.2936